MATHEMATICAL BIOSCIENCES
AND ENGINEERING
Volume **10**, Number **3**, June **2013**

doi:10.3934/mbe.2013.10.591

pp. **591–608**

A PARTIAL DIFFERENTIAL EQUATION MODEL OF METASTASIZED PROSTATIC CANCER

Avner Friedman

Department of Mathematics, The Ohio State University
Columbus, OH 43210, USA

Harsh Vardhan Jain

Department of Mathematics, Florida State University
Tallahassee, FL 32308, USA

Abstract. Biochemically failing metastatic prostate cancer is typically treated with androgen ablation. However, due to the emergence of castration-resistant cells that can survive in low androgen concentrations, such therapy eventually fails. Here, we develop a partial differential equation model of the growth and response to treatment of prostate cancer that has metastasized to the bone. Existence and uniqueness results are derived for the resulting free boundary problem. In particular, existence and uniqueness of solutions for all time are proven for the radially symmetric case. Finally, numerical simulations of a tumor growing in 2-dimensions with radial symmetry are carried in order to evaluate the therapeutic potential of different treatment strategies. These simulations are able to reproduce a variety of clinically observed responses to treatment, and suggest treatment strategies that may result in tumor remission, underscoring our model's potential to make a significant contribution in the field of prostate cancer therapeutics.

1. **Introduction.** The prostate is an exocrine gland of the male reproductive system, which produces an alkaline fluid that is one of the key components of semen [30]. Unfortunately, the prostate is highly susceptible to cancer, with prostate cancer (CaP) being second most common type of cancer affecting men in the United States. In recent years, there have been more than 200,000 new cases diagnosed annually in the United States, resulting in over 30,000 deaths per year [7]. Thus, CaP is a major public health challenge.

Healthy prostate cells, as well as CaP cells require male sex hormones called androgens for their survival and proliferation. The principle androgen is testosterone, which is produced in the testes. Upon entering a CaP cell, testosterone is mostly converted to its more active metabolite, dihydrotestosterone (DHT). Both testosterone and DHT bind to and activate intracellular androgen receptors, that result in growth, survival and proliferation cues [12, 28]. For this reason, cases of advanced or metastasized prostate cancer are treated with hormone therapeutic strategies

2010 *Mathematics Subject Classification.* Primary: 92C40, 92C50; Secondary: 37N25.

Key words and phrases. Androgen ablation, free boundary problem, mathematical model, prostate cancer, PSA.

that result in androgen ablation. This treatment works well initially, but eventually cancer cells may mutate into an androgen-independent phenotype, resulting in resistance and treatment failure [9].

Prostatic cells, healthy and cancerous, produce a proteolytic glycoprotein called prostate-specific antigen (PSA), that aids in semen motility. Consequently, its blood serum levels are believed to be correlated with cancer load, with increases in PSA levels indicative of an increasing tumor burden and decreases in PSA levels indicative of a decreasing tumor burden. Therefore, serum PSA concentration in CaP patients is closely monitored by clinicians, and androgen ablation may be scheduled based on its values [13, 14].

We recently developed a biochemically-based mathematical model of advanced CaP [21] in order to gain a better understanding of the consequences of current clinical care and to investigate therapeutic options that might delay or prevent the emergence of resistance to androgen ablation therapy. While a number of mathematical models [8, 17, 18, 19, 20, 26] aimed at investigating the therapeutic potential of hormone treatment in CaP have been proposed previously, ours was the first to include a number of patient-specific personalized parameters allowing us to capture the heterogeneity that is a hallmark of prostate cancer. Model simulations were able to reproduce a variety of clinically observed outcome for patients under different chemotherapeutic schedules. In a subsequent paper [22], we reduced the model (by means of a singular perturbation analysis) to a simple system of three coupled ordinary differential equations. With this simpler model, we were able to predict, under some assumptions, therapy schedules that lead to a complete cure, or total failure depending on the values of the personalized parameters of patients.

The models in [21, 22] were based on systems of ordinary differential equations. In the present work, we are concerned with a situation where the cancer has spread into the bone, which is one of the most common sites of metastasis for CaP [29]. Here, the cancer begins to grow as a solid tumor. This spatial situation calls for a spatial model that needs to be formulated in terms of partial differential equations in a tumor region $\Omega(t)$, which varies with t.

We shall use as a starting point, the simplified approach of [22] and thus include in our model of metastatic CaP treatment: prostate cancer cells N; mutated cancer cells M; healthy bone marrow cells H; androgen concentration A; and PSA concentration P. The cells N, M and H are assumed to satisfy hyperbolic conservation laws while the dynamics of A are governed by a diffusion equation. P is taken to be proportional to the total number of cells and will determine the treatment schedule. Given any initial tumor $\Omega(0)$, with a smooth boundary $\Gamma(0)$, we shall prove existence and uniqueness of the free boundary problem for N, M, H, A and P with a smooth free boundary $\Gamma(t)$ for a small time interval $0 \le t \le T$; in the case of radially symmetric initial data, we shall prove existence and uniqueness of solutions for all $t > 0$, with a continuously differentiable free boundary $\Gamma(t)$ and radius of the tumor $r = R(t)$. Finally, we will present numerical simulations illustrating the cases of a complete cure or total failure with anti-androgen therapy.

2. **Model development.**

We consider CaP that has metastasized and is occupying a region $\Omega(t)$ at time t. We introduce the following variables in our model:

N = Density of androgen-dependent CaP cells,
M = Density of mutated CaP cells,
H = Density of healthy bone (non-prostatic) cells,

D = Density of dead cells,
A = Concentration of androgens,
P = Concentration of PSA.

CaP is treated with androgen ablation based on PSA concentration, where the therapy is switched 'on' if PSA rises above a critical threshold, say P_0. This results in a decreased rate of androgen production, coupled with an inhibition of intracellular androgen receptors. In our model, we account for androgen ablation by assuming a reduction in the normal rate of androgen production by a factor of $1 + \lambda f(P)$, say, where $f(\cdot)$ is a smooth approximation of the Heaviside function $H(P - P_0)$. Thus, $f(P)$ simulates the application of therapy, so that $f(P) = 1$ corresponds to therapy 'on' and $f(P) = 0$ corresponds to therapy 'off'. We assume that the cells are uniformly distributed in $\Omega(t)$, so that:

$$N + M + H + D = \text{ constant } (= 1, \text{ say}) \text{ in } \Omega(t) \tag{1}$$

Hence, as a result of cellular proliferation and the removal of dead cells, there is a movement of cells within $\Omega(t)$, that is itself evolving in time; we denote the velocity of this movement by $\vec{v} = \vec{v}(x, t)$. The following equations model the dynamics of cells, androgen and PSA in $\Omega(t)$.

$$\frac{\partial N}{\partial t} + \nabla \cdot (\vec{v}N) = \underbrace{K_N(A)N}_{\substack{\text{androgen-dep-}\\ \text{endant growth}}} - \underbrace{K_{NM}(A)N}_{\text{mutation}} - \underbrace{\mu N}_{\text{death}}, \tag{2}$$

$$\frac{\partial M}{\partial t} + \nabla \cdot (\vec{v}M) = \underbrace{K_M(A)M}_{\substack{\text{androgen-me-}\\ \text{diated growth}}} + \underbrace{K_{NM}(A)N}_{\text{mutation}} - \underbrace{\mu M}_{\text{death}}, \tag{3}$$

$$\frac{\partial H}{\partial t} + \nabla \cdot (\vec{v}H) = \underbrace{K_H H \left(1 - \frac{N + M + H}{K_0}\right)}_{\text{proliferation with contact-inhibition}} - \underbrace{\mu H}_{\text{death}}, \tag{4}$$

$$\frac{\partial D}{\partial t} + \nabla \cdot (\vec{v}D) = \mu(N + M + H) - \min\{0, K_N(A)\} N - \min\{0, K_M(A)\} M - \underbrace{\mu_D D}_{\text{removal}}, \tag{5}$$

$$\frac{\partial A}{\partial t} - D_A \nabla^2 A = \underbrace{\frac{\lambda_A}{1 + \lambda f(P, t)}}_{\substack{\text{drug-inhibited}\\ \text{production}}} - \underbrace{\mu_A A}_{\text{decay}} - \underbrace{\lambda_0 (N + M) A}_{\substack{\text{consumption by}\\ N \text{ and } M}}, \tag{6}$$

$$P = P(t) = \int_{\Omega(t)} (N + M) dx. \tag{7}$$

We recall that androgen-dependent CaP cells (like healthy prostatic epithelial cells) require androgens for their survival and proliferation. Therefore, N cell growth rate $K_N(A)$ is assumed to be an increasing and saturating function of A, where $K_N(A) < 0$ if A is small, and $K_N(A) = \text{constant} > 0$ if A is large, that is, if $A > A_0$, a level corresponding to physiologically normal androgen concentration. Following [21, 22], the rate of mutation from N to M cells is taken as $K_{NM}(A) = K_N(A)\alpha_{mut}$, where α_{mut} represents the probability of a cell phenotype N mutating as a consequence of aberrant DNA replication during proliferation. As in previous studies [18, 19, 20, 22], the growth rate $K_M(A)$ of M cells is taken to be

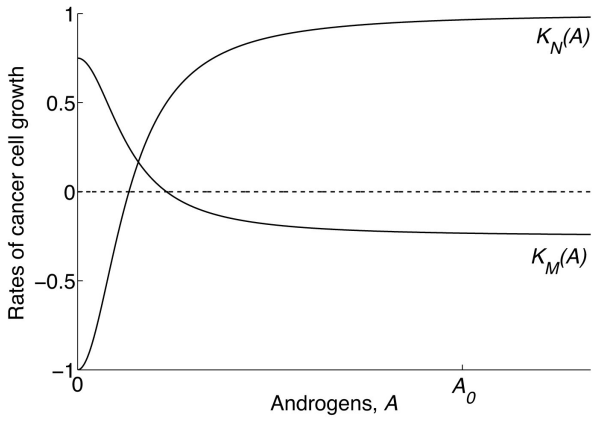

FIGURE 1. Assumed androgen dependent cell growth rate ($K_N(A)$) and castration-resistant cell growth rate ($K_M(A)$). Above a critical threshold of androgen concentration (A_0), androgen dependent cells have a positive proliferation rate, while castration-resistant cells have a negative rate of growth. At low androgen concentrations, castration resistant cells proliferate while androgen dependent cells undergo apoptosis.

a decreasing function of A. That is, M cells are assumed to be androgen-repressed, so that they have a negative growth rate in the presence of androgens. Note that Androgen-repressed castration-resistant cells have been isolated from human tumors [32]. Figure 1 shows typical profiles of $K_N(A)$ and $K_M(A)$.

In equations (2)-(4), μ is the natural death rate of cells, and is assumed to be equal for all cell types. Note that we have separately accounted for the death rates of CaP cells due to high or low levels of androgens. In equation (4), bone marrow cells are assumed to proliferate at a maximum rate K_H. Contact inhibition for healthy cells due to over-crowding is also incorporated in our model, so that as the total number of cells increases, the proliferation rate of H cells decreases. As can be seen, in the absence of CaP cells, H cells achieve a steady-state of $K_0(1-\mu/K_H)$. Under drug-free conditions, androgens are also assumed to be produced at a constant rate λ_A, while the effect of androgen ablation on A has already been discussed previously. Androgens are further assumed to undergo natural decay at a rate μ_A. When CaP cells are present, they are assumed to take up androgens at a constant rate λ_0. Finally, for simplicity, PSA concentration P is taken to be proportional to the total number of CaP cells.

Note that, in healthy conditions, that is, in the absence of CaP cells and androgen ablation therapy, the steady state concentration of androgens is given by $A_0 = \lambda_A/\mu_A$. From equation (1), we have:

$$D = 1 - N - M - H \tag{8}$$

By adding equations (2)-(5), and using the above expression for D, we obtain the following equation for $\nabla \cdot \vec{v}$:

$$\nabla \cdot \vec{v} = -\ \mu_D(1 - N - M - H)\ +\ \max\{0, K_N(A)\}\, N\ +\ \max\{0, K_M(A)\}\, M \tag{9}$$

$$+ K_H H\left(1 - \frac{N+M+H}{K_0}\right)$$
$$\equiv G(N, M, H, A).$$

In what follows, we may replace equation (5) by (2). Indeed, if N, M, H and $\vec{v}$ solve the system (2)-(4) and (2), and we define D by (8), then it can easily be seen that D satisfies equation (5).

We assume in our model that the tumor host tissue (that is, bone) is a porous medium, so that by Darcy's Law,

$$\vec{v} = -\nabla\sigma, \tag{10}$$

where σ is the isotropic pressure of the moving cells. Then, by equation (2),

$$\nabla^2\sigma = -G(N, M, H, A). \tag{11}$$

We next assume that the free boundary $\Gamma(t)$ of the tumor region $\Omega(t)$ is moving with velocity $\vec{v}$, that is,

$$V_n = \vec{v}\cdot\vec{n}, \tag{12}$$

where $\vec{n}$ is the outward normal to $\Gamma(t)$, and V_n is the velocity of $\Gamma(t)$ in the direction $\vec{n}$.

We complete the above system by prescribing the boundary conditions

$$\begin{aligned} \sigma &= \gamma K,\ \gamma > 0, \\ \text{and } A &= A_0/(1+\lambda f(P)) \text{ on } \Gamma(t), \end{aligned} \tag{13}$$

and initial conditions

$$\begin{aligned} \Omega(t=0) &= \Omega^0,\ \Gamma(t=0) = \Gamma^0, \\ N(x, t=0) &= N^0(x),\ M(x, t=0) = M^0(x) \\ H(x, t=0) &= H^0(x),\ \text{and } A(x, t=0) = A^0(x),\ \text{in } \Omega^0, \end{aligned} \tag{14}$$

where K is the mean curvature ($K = 1/R$, if $\Gamma(t)$ is a sphere of radius R), and we assume that

$$\begin{aligned} A^0(x) &= \text{constant} = A_0 \text{ on } \Gamma^0, \\ A^0, N^0, M^0, H^0 &\geq 0,\ \text{and } N^0 + M^0 + H^0 \leq 1 \text{ in } \Omega^0. \end{aligned} \tag{15}$$

Note that since the free boundary is a characteristic surface for the hyperbolic equations (2)-(5), no boundary conditions need to be assigned for the variables N, M, H and D.

Definition 2.1. We refer to equations (2)-(4), (6)-(7), and (2)-(15) describing CaP growth and treatment as system (P).

Theorem 2.2. *For any smooth solution of the system (P), there holds:*

$$A \geq 0,\ N \geq 0,\ M \geq 0, H \geq 0,\ \textit{and } N + M + H \leq 1 \textit{ in } \Omega(t),\ \forall\, t. \tag{16}$$

Proof. The inequality $A \geq 0$ follows by the maximum principle. The inequalities $N \geq 0$, $M \geq 0$, $H \geq 0$ follow by integrating each of these functions along characteristics. Next, if we define D by equation (8), then, as remarked earlier, D satisfies equation (5). Hence, by integrating this equation along characteristics, we get $D \geq 0$, so that $N + M + H = 1 - D \leq 1$. □

3. **Existence and uniqueness.** In this section, we shall prove the existence and uniqueness of a smooth solution of system (P) on a small time interval when the tumor boundary and initial conditions are sufficiently smooth. For the special case of a radially symmetric tumor, we shall prove the existence and uniqueness of a smooth solution for all time.

We begin by introducing the following notation: For any vector $\beta = (\beta_0, \cdots, \beta_N)$, β_i integers ≥ 0, set $|\beta| = \beta_0 + \beta_1 + \cdots + \beta_N$ and

$$D^\beta \varphi \;=\; D^\beta_{(x,t)}\varphi \;=\; \frac{\partial^{|\beta|}\varphi}{(\partial t)^{\beta_0}(\partial x_1)^{\beta_1}\cdots(\partial x_N)^{\beta_N}}.$$

For any $0 < \alpha_1, \alpha_2, \alpha < 1$, m integer ≥ 0, define

$$\|\varphi\|_0 \;=\; \sup|\varphi|,\;\; \|\varphi\|_m \;=\; \sum_{|\beta|\leq m} \|D^\beta\varphi\|_0,$$

$$[\varphi]_{\alpha_1,\alpha_2} \;=\; \sup \frac{|\varphi(x,t)-\varphi(y,\tau)|}{|x-y|^{\alpha_1}+|t-\tau|^{\alpha_2}},$$

$$\|\varphi\|_{m+\alpha_1,m+\alpha_2} \;=\; \|\varphi\|_0 + \sum_{|\beta|=m} [D^\beta\varphi]_{\alpha_1,\alpha_2}, \tag{17}$$

$$\|\varphi\|_{3+\alpha,(3+\alpha)/3} \;=\; \|\varphi\|_0 + [D_x^3\varphi]_{\alpha,\alpha/3} + [D_t\varphi]_{\alpha,\alpha/3}, \tag{18}$$

where the regions where these norms are taken will be defined, as needed, later on.

We note that the right-hand side of (17) dominates $\|\varphi\|_m$, so that by adding this norm to the right-hand side of (17) we obtain a new norm which is equivalent to $\|\varphi\|_{m+\alpha_1,m+\alpha_2}$. Similarly (cf. [5]), the right-hand side of (18) dominates

$$[D_x^2\varphi]_{0,(1+\alpha)/3} + [D_x\varphi]_{0,(2+\alpha)/3}.$$

We say that $\varphi \in C^{m+\alpha_1,m+\alpha_2}$ if $\|\varphi\|_{m+\alpha_1,m+\alpha_2} < \infty$. Similarly we define the notions $\varphi \in C^{3+\alpha,(3+\alpha)/3}$, $\varphi \in C^{2+\alpha,(2+\alpha)/3}$.

We assume that

$$\Gamma^0 \in C^{m+4+\alpha}, \tag{19}$$

where $0 < \alpha < 1$ and $m = 0$ or $m = 1$. Denote by s a variable point in Γ^0 and by $\vec{n}(s)$ the outward normal to Γ^0 at s. We shall write $\Gamma(t)$ in the form

$$\Gamma(t) \;=\; \{s + \rho(s,t)\vec{n}(s)\}. \tag{20}$$

Let $d = d(x) = d(x,\Gamma^0)$ denote the signed distance from x to Γ^0 ($d(x) > 0$ if x is outside Ω^0). Then we can express points x near Γ^0 in the form

$$x \;=\; s + d\,\vec{n}(s),$$

where s is uniquely determined by x.

It will be convenient to use local coordinate transformation to flatten the free boundary. We take local coordinates $y' = (y_1, y_2)$ near 0, about a point s_0 in Γ^0, so that $s = S(y_1, y_2)$ for $|s - s_0|$ small. Then, for x near s_0,

$$x \;=\; S(y_1,y_2) + (\rho(s,t) + y_3)\vec{n}\,(S(y_1,y_2)),$$

where $y_3 = d(x,\Gamma^0) - \rho(s,t)$. This defines a local mapping $y \to x$ from a neighborhood of the origin in $\mathbb{R}^3$ into an $\mathbb{R}^3$-neighborhood of s_0 such that $x \in \Gamma(t)$ corresponds to $(y', 0)$. While this change of variables makes the PDE system (P) more complicated, the analysis will actually be simplified since the free-boundary is locally flat.

We assume that

$$N^0, M^0, H^0, A^0 \in C^{m+1+\alpha}(\overline{\Omega}^0), \tag{21}$$

and that

$K_N(A), K_{NM}(A), K_M(A)$ and $f(P)$ are uniformly Hölder continuous, exponent α. (22)

Theorem 3.1. *Under the conditions (19)-(22), the system (P) has a unique solution for some interval $0 \le t \le T$ $(T > 0)$ such that*

$$D_s D^m_{(s,t)}\rho \in C^{3+\alpha,(3+\alpha)/3}(\Gamma^0 \times [0,T]), \tag{23}$$

$$D^2_x D^m_{(x,t)}\sigma \in C^{\alpha,\alpha/3}(\mathbb{R}^3 \times [0,T]), \tag{24}$$

and N, M, H, A can be extended into functions in $C^{m+1+\alpha,m+1+\alpha/3}(\mathbb{R}^3 \times [0,T])$.

Proof. We introduce the space Y of functions $X = (N, M, H, A)$ in $C^{m+\alpha,m+\alpha/3}(\mathbb{R}^3 \times [0,T])$ with norm

$$\|X\|_T = \|X\|_{C^{m+\alpha,m+\alpha/3}(\mathbb{R}^3\times[0,T])},$$

and a closed L-ball

$$Y_L = \{X : \|X\|_T \le L\},$$

where L is a fixed but large enough positive constant.

For any X in Y_L, we define G as in (2) and solve the Hele-Shaw problem

$$\begin{aligned} \triangle\sigma &= -G \text{ in } \Omega(t), \\ \sigma &= \gamma K, \ \frac{\partial\sigma}{\partial\vec{n}} = -V_n \text{ on } \Gamma(t) \end{aligned} \tag{25}$$

for $0 \le t \le T$. As shown in [5], this system has a unique solution $(\sigma, \Gamma(t))$ in the class (23), (24).

Setting $v = -\nabla\sigma$, we next solve the system, in $\{\Omega(t), 0 \le t \le T\}$

$$\begin{aligned} \frac{\partial\overline{N}}{\partial t} + \nabla\cdot(\vec{v}\overline{N}) &= K_N(\overline{A})\overline{N} - K_{NM}(\overline{A})\overline{N} - \mu\overline{N} \\ \frac{\partial\overline{M}}{\partial t} + \nabla\cdot(\vec{v}\overline{M}) &= K_M(\overline{A})\overline{M} + K_{NM}(\overline{A})\overline{N} - \mu\overline{M} \\ \frac{\partial\overline{H}}{\partial t} + \nabla\cdot(\vec{v}\overline{H}) &= K_H\overline{H}\left(1 - \frac{\overline{N}+\overline{M}+\overline{H}}{K_0}\right) - \mu\overline{H} \\ \frac{\partial\overline{A}}{\partial t} - D_A\nabla^2\overline{A} &= \frac{\lambda_A}{1+\lambda f(P)} - \mu_A\overline{A} - \lambda_0(\overline{N}+\overline{M})\overline{A}, \end{aligned}$$

with the prescribed initial and boundary conditions, and where P is defined by (7). We then extend the components of the solution to functions in $\mathbb{R}^n \times [0,T]$, in a specific way; for example along normals to $\Gamma(t)$ with a fixed cutoff function.

As argued in [5], the function $\overline{X} = (\overline{N}, \overline{M}, \overline{H}, \overline{A})$ is in $C^{m+1+\alpha,m+1+\alpha/3}$, which is a higher regularity class than the initially given regularity class of X. We can then proceed with a fixed point argument, showing that the mapping $W : X \to \overline{X}$ maps Y_L into itself, and is a contraction provided T is small enough. This completes the proof of Theorem 3.1. □

We next consider the case where Ω^0 is a sphere of radius R_0, and N^0, M^0, H^0, A^0 are radially symmetric functions in C^1.

Theorem 3.2. *Under the above assumptions, there exists a unique radially symmetric solution of the system (P) for all* $0 \leq t < \infty$ *with free boundary* $r = R(t)$ *in* C^1.

Proof. The proof of Theorem 3.2 is somewhat different from the proof of Theorem 3.1. We introduce functions $X = (N, M, H, A)$ with the uniform C^1-norm (instead of $C^{m+\alpha}$), and follow the same outline as before, but with somewhat simpler norm estimates. The reason for this different approach is that in order to extend the local in-time solution step-by-step, it is easier to work with the C^1-norm. Arguing along similar lines as in [10], we establish a priori estimates

$$R(t) \geq \text{constant} \ > 0,$$
$$|\dot{R}(t)| \leq \text{constant} \ < \infty,$$

for any interval $0 \leq t < T$, where the solution exists, and the constants are bounded functions of T, for any $T > 0$. Hence, the solution can be extended for all $t > 0$. □

Remark 1. Consider the case when the tumor has metastasized into several regions $\Omega_i(t)$. Then, in each region we have a system for N_i, M_i, H_i, D_i, $\vec{v}_i$ and A_i as in system (P), and they are all coupled by the following expression for PSA:

$$P = \sum_i \int_{\Omega_i(t)} (N_i + M_i) dx.$$

The proofs of Theorems 3.1 and 3.2 easily extend to this case.

Remark 2. The therapy application function $f(P)$ appearing in equation (6) may also depend explicitly on time t if, for instance, androgen ablation is administered continuously or on an intermittent schedule with fixed period on and off therapy. The analysis in section 3 remains unaltered if $f(P, t)$ is Hölder continuous in t, and in the radial case, if it is simply continuous in t. In the numerical simulations that follow, we will consider $f(P, t)$ with the above properties, as well functional forms that are clinically more relevant.

4. **Numerical simulations.** In this section, we simulate tumor response to continuous and intermittent androgen ablation, with intermittent therapy based on different scheduling strategies. Simulations are carried for a tumor growing in 2-dimensions with radial symmetry. In all results that follow, the growth rate $K_N(A)$ of N cells is kept fixed, while the growth rate $K_M(A)$ of M cells is varied to illustrate the various possible outcomes of therapy application. The variables N, M, H A and P are cast in dimensionless terms, while time t is measured in days, and tumor radius $R(t)$ measured in centimeters. This corresponds to the typical time-scale of CaP cell growth and length-scale on which the cancer is clearly distinguishable in bone scans. The initial diameter of the tumor is taken to be 1 cm, and uniform initial densities of $N = N^0$, $M = M^0$ and $H = H^0$ cells are presumed.

We first simulate the case when a tumor is treated with continuous androgen ablation. Therapy is started once PSA reaches a critical threshold $P_0 = 5$, at day $t_0 = 75$. Continuous therapy is simulated by taking $f(P, t)$ to be a smooth approximation to the Heaviside Function $H(t > t_0)$ in equation (6). As can be seen from Figure 2A, PSA declines rapidly on therapy application, attaining a minimum of < 1 at day 250, before increasing again due to the emergence of castration-resistance. A plot of androgen concentration averaged over the tumor domain in Figure 2C reveals

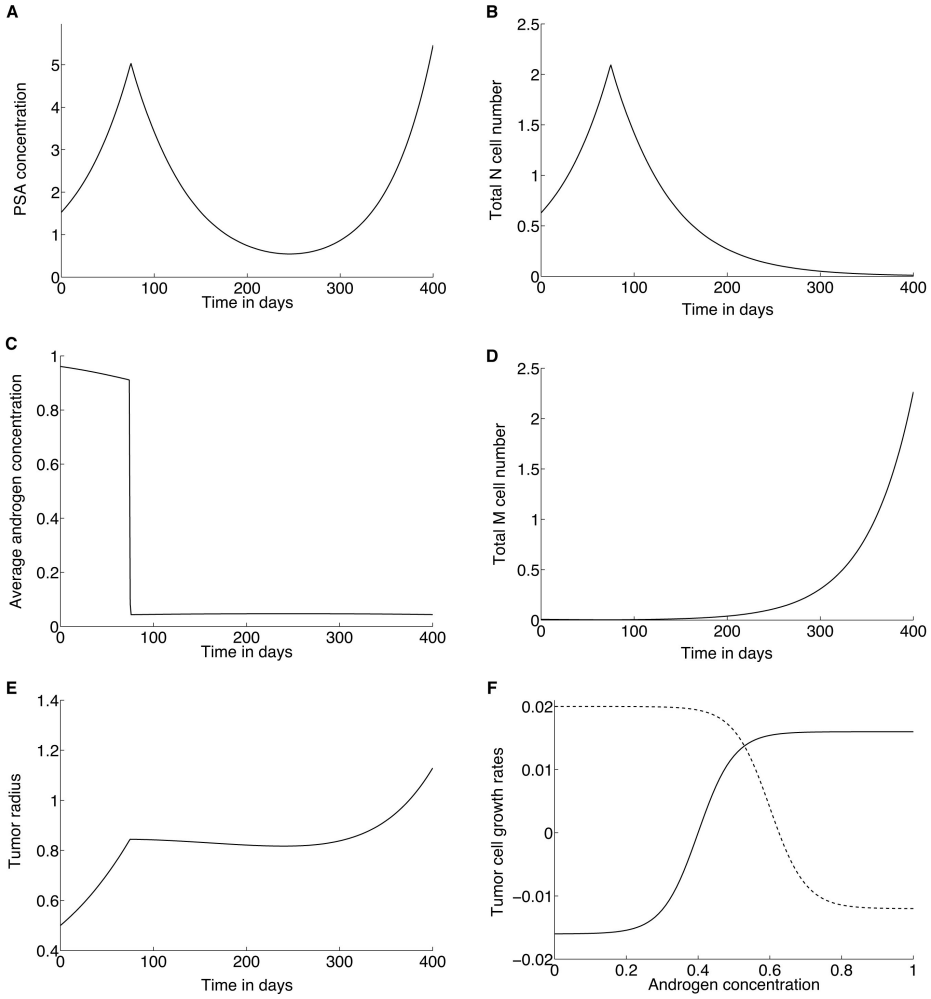

FIGURE 2. Numerical predictions of cancer response to continuous androgen ablation applied starting on day 75. Figure shows time-courses of **A**, PSA concentration ($P(t)$), **B**, total number of androgen dependent cells ($=\int_{\Omega(t)} N(r,t)dr$), **C**, average androgen concentration ($=\int_{\Omega(t)} A(r,t)dr/\int_{\Omega(t)} 1dr$), **D**, total number of castration resistant cells ($=\int_{\Omega(t)} M(r,t)dr$), and **E** tumor radius ($R(t)$). **F**, Growth rates of androgen dependent cells (solid curve) and castration resistant cells (dashed curve).

that when therapy is applied, the average androgen concentration falls rapidly to a low minimum value. Time-courses of N and M cell numbers integrated over the entire tumor domain are plotted in Figures 2B and 2D, respectively. On therapy application, N cells decline rapidly to 0, while M cells grow exponentially. Prior to therapy application N cells dominate the tumor, and their proliferation drives tumor radius ($R(t)$) growth during this period (Figure 2E). When therapy is first

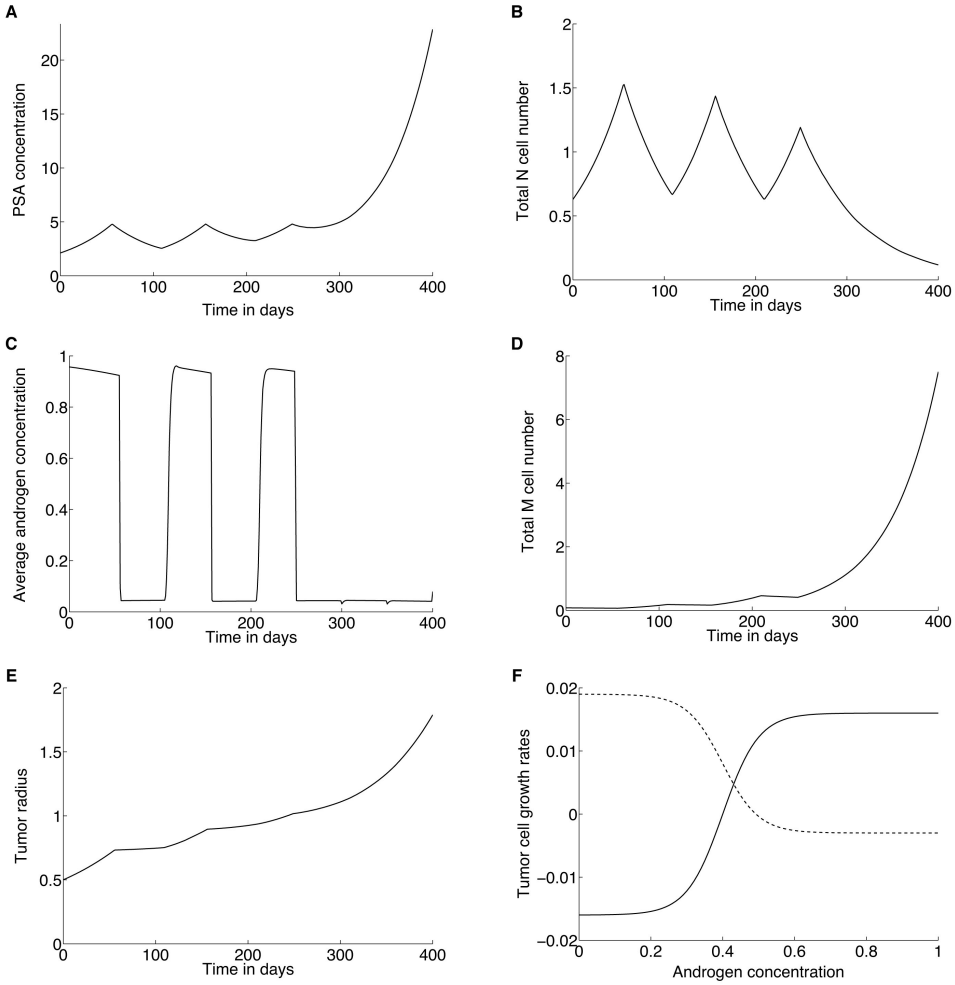

FIGURE 3. Numerical illustration of the case when intermittent androgen ablation is predicted to fail. Intermittent therapy is based on the schedule that treatment is reinstituted with a PSA of 5, and remains on for 2 months. Figure shows time-courses of **A**, PSA concentration ($P(t)$), **B**, total number of androgen dependent cells ($=\int_{\Omega(t)} N(r,t)dr$), **C**, average androgen concentration ($=\int_{\Omega(t)} A(r,t)dr/\int_{\Omega(t)} 1dr$), **D**, total number of castration resistant cells ($=\int_{\Omega(t)} M(r,t)dr$), and **E** tumor radius ($R(t)$). **F**, Growth rates of androgen dependent cells (solid curve) and castration resistant cells (dashed curve).

applied, the $R(t)$ experiences a transient decline due to N cell death, before increasing exponentially as a result of M cell dominance under androgen ablation conditions. Figure 2F shows a plot of the assumed growth rates of N (solid curve) and M (dashed curve) cells.

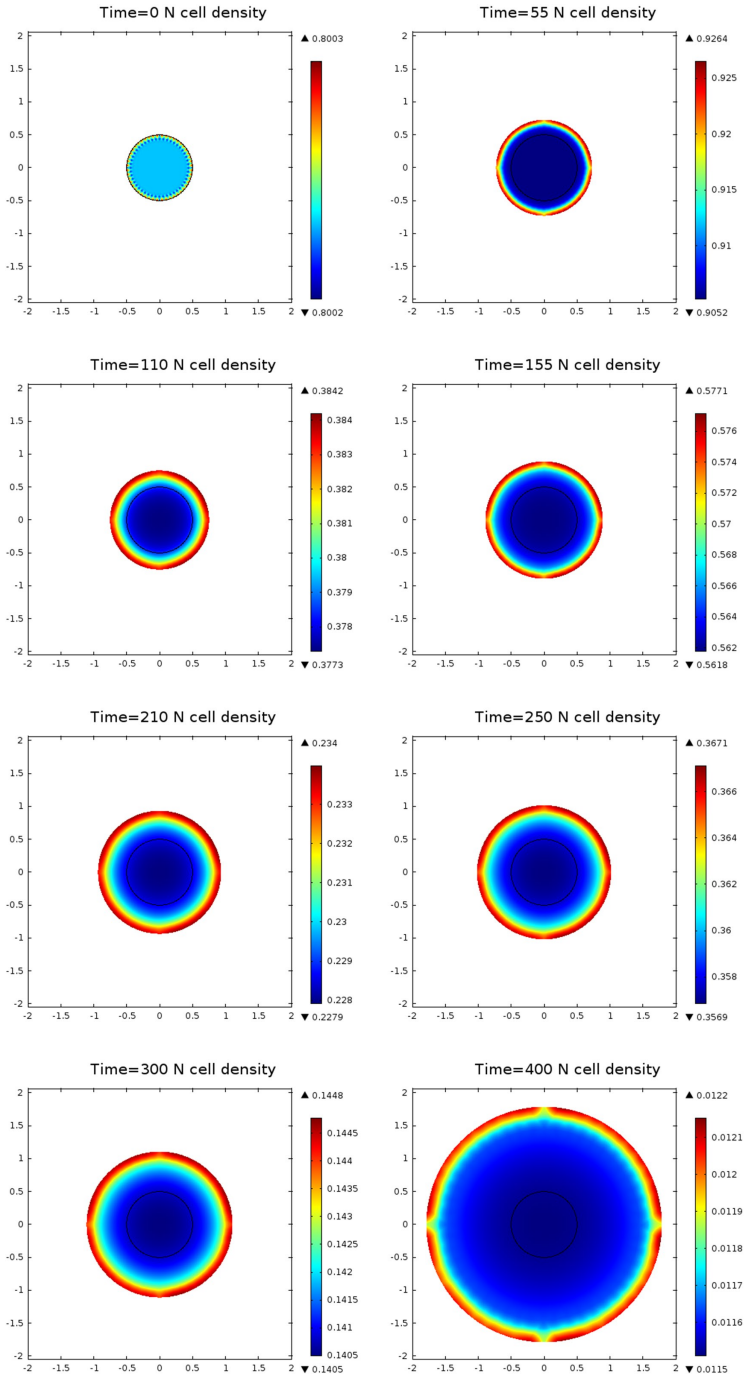

FIGURE 4. Surface plots of androgen dependent (N) cell density corresponding to the intermittent therapy in Figure 3, taken at initial time ($t = 0$), when therapy is switched on ($t = 55, 155, 250$), when therapy is switched off ($t = 110, 210$) and when castration resistance has emerged ($t = 300, 400$).

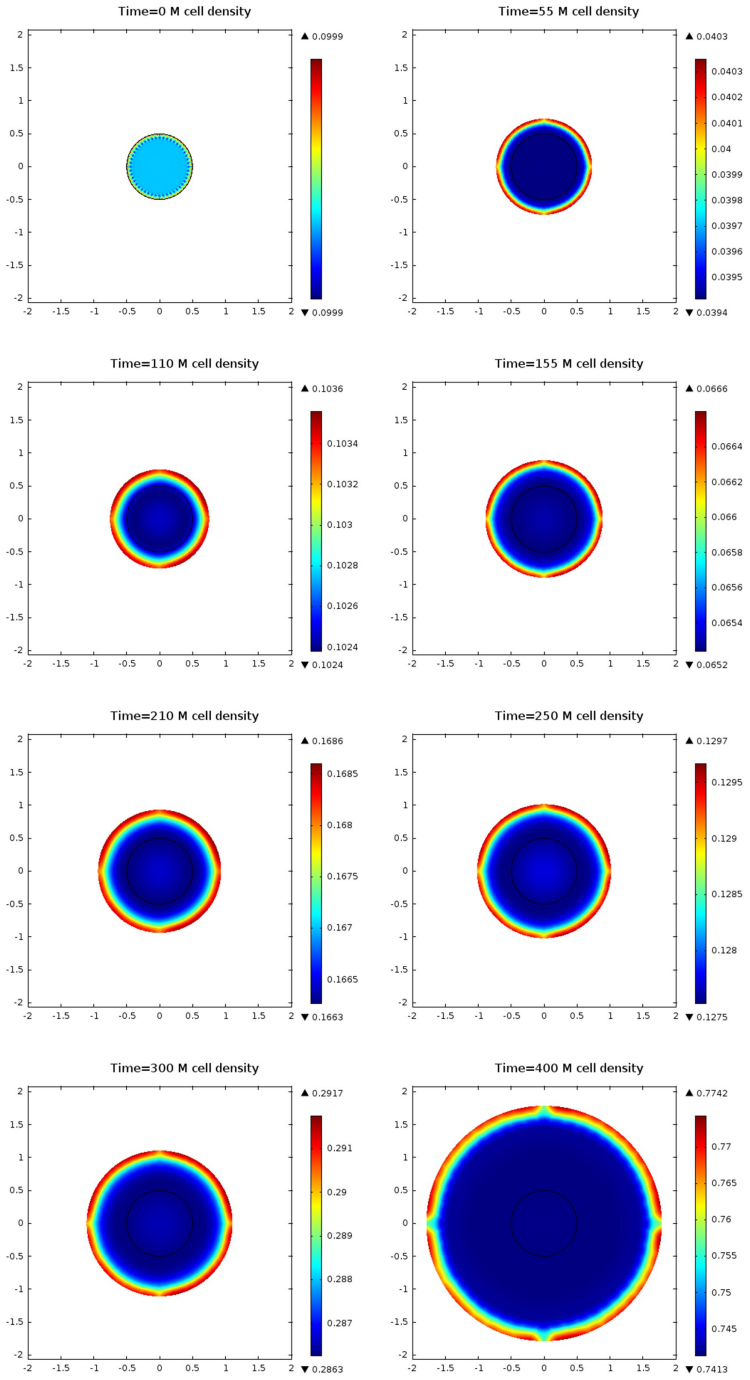

FIGURE 5. Surface plots of castration resistant (M) cell density corresponding to the intermittent therapy in Figure 3, taken at initial time ($t = 0$), when therapy is switched on ($t = 55, 155, 250$), when therapy is switched off ($t = 110, 210$) and when castration resistance has emerged ($t = 300, 400$).

We next simulate a tumor that is treated with intermittent androgen ablation, based on the schedule that therapy is reinstituted with a PSA of 5, and remains on for 2 months. Similar schedules have been considered in a clinical setting [14]. The schedule can be visualized from the time-course of the averaged androgen concentration in Figure 3C, with androgen concentration near 0.9 indicating periods off therapy, and concentrations below 0.1 indicating periods on therapy. With tumor cell growth rates fixed as shown in Figure 3F, intermittent therapy is predicted to fail in the third cycle, as can be seen from a time-course of PSA in Figure 3A. The tumor radius now grows unchecked (Figure 3E), driven by M cell proliferation (Figure 3D). To illustrate the spatial structure of the tumor, surface plots of N and M cell densities are shown in Figures 4 and 5 respectively, at the following times: $t = 0$, $t = 55, 155, 250$ when therapy is switched on, $t = 110, 210$ when therapy is switched off and $t = 300, 400$ by which times castration resistance has emerged. N cell density alternates between periods of growth ($t \in [0, 55] \cup [110, 155] \cup [210, 250]$) and decay in between and for $t \geq 250$, while the growth and decay periods for M cells are reversed. Further, the region of maximum proliferation, and hence maximum cell density, is predicted to be at the rim of the tumor.

The above intermittent schedule may also result in periodic cycling of PSA, dependent on N and M cell proliferation and death rates. If tumor cell growth rates are as shown in Figure 6F, the total numbers of both N and M cells appear to settle to periodic oscillations (Figures 6B and 6D, respectively), so that the resultant PSA concentration is predicted to oscillate between a maximum of 5 and a minimum of 2. Figure 6E reveals that the tumor radius experiences periods of growth during periods off therapy due to N cell proliferation, and transient declines during periods on therapy due to N cell death and a low density of M cells.

In all the above cases, the initial M cell density is taken to have a low value of < 0.1, as compared to the initial N cell density, which is taken to be > 0.7. We finally illustrate a case where an appropriately chosen intermittent schedule may result in a cure, even in the case when a large number of M cells are present in the tumor initially. We have previously shown [22] that for a spatially uniform tumor, when the growth rates of N and M cells are such that $G_{\min} = \left| \dfrac{\min\{0, K_M(A)\}}{\max\{0, K_M(A)\}} \right| < \left| \dfrac{\min\{0, K_N(A)\}}{\max\{0, K_N(A)\}} \right| = G_{\max}$, then an intermittent schedule in which the ratio of times off and on therapy in each cycle lies between $G_{\min}$ and $G_{\max}$ will result in a cure. Figure 7 reveals that the same result is observed for the spatially inhomogenous case, as evidenced by an overall decline in PSA concentration (Figure 7A), and eventual decline in tumor radius (Figure 7E). Now, the initial density of M cells is taken to be as high as 0.3, with tumor cell growth rates chosen such that the above condition is satisfied (see Figure 7F, $G_{\max} = 1$ and $G_{\min} = 0.16$). In each cycle of therapy, the time on therapy is fixed at 2 months, while the time off therapy fixed at 40 days, so that (Time off therapy)/(Time on therapy) = 0.67.

5. **Discussion.** Biochemically failing metastatic prostate cancer is treated with androgen ablation. However, treatment failure is nearly universal due to the emergence of castration resistant cells that continue to proliferate despite blocking the production of androgens and their receptors. It has been hypothesized that androgen deprived conditions create a positive selection bias for castration resistant cells that may exist as a small population prior to therapy application. Consequently,

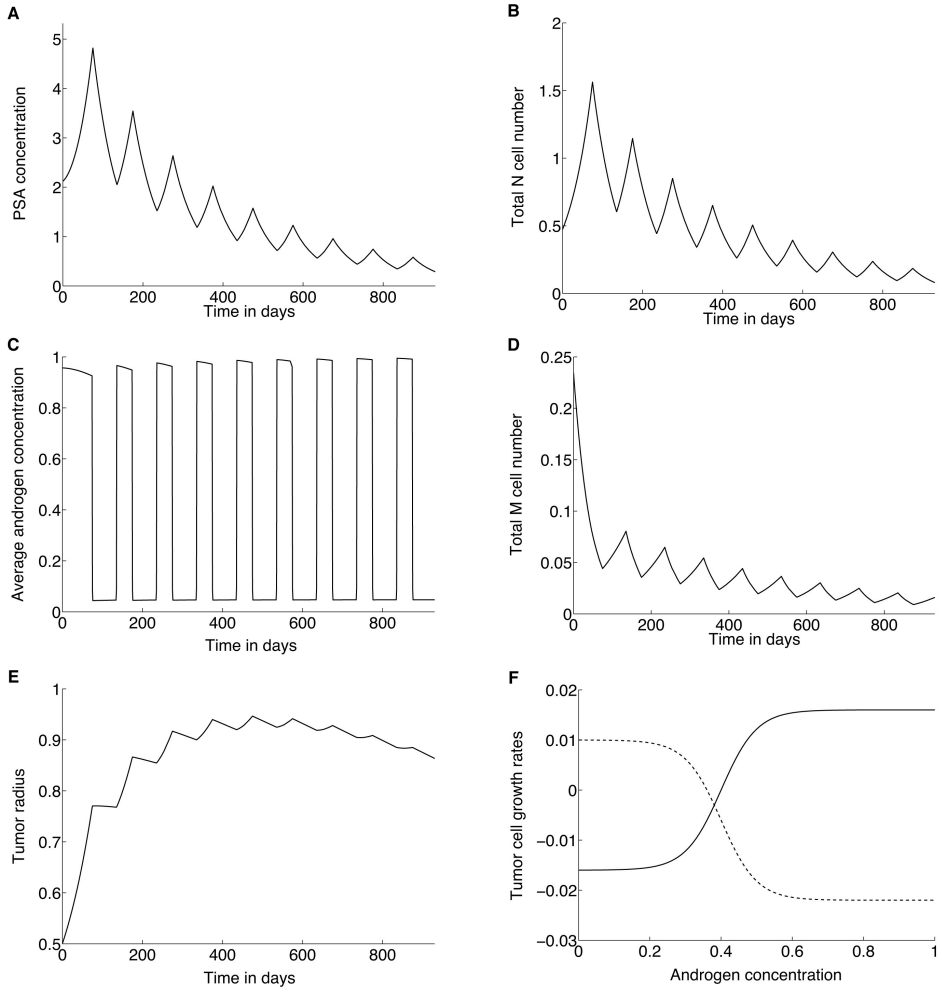

FIGURE 6. Numerical illustration of the case when intermittent androgen ablation is predicted to result in infinite cycling. Intermittent therapy is based on the schedule that treatment is reinstituted with a PSA of 5, and remains on for 2 months. Figure shows time-courses of **A**, PSA concentration ($P(t)$), **B**, total number of androgen dependent cells ($=\int_{\Omega(t)} N(r,t)dr$), **C**, average androgen concentration ($=\int_{\Omega(t)} A(r,t)dr/\int_{\Omega(t)} 1dr$), **D**, total number of castration resistant cells ($=\int_{\Omega(t)} M(r,t)dr$), and **E** tumor radius ($R(t)$). **F**, Growth rates of androgen dependent cells (solid curve) and castration resistant cells (dashed curve).

intermittent therapy application has been proposed as a means to delay the onset of resistance. In order to simulate tumor growth and treatment, and to investigate the therapeutic potential of various treatment strategies, we developed and analyzed a model of CaP that has metastasized to the bone, and is growing as a solid tumor.

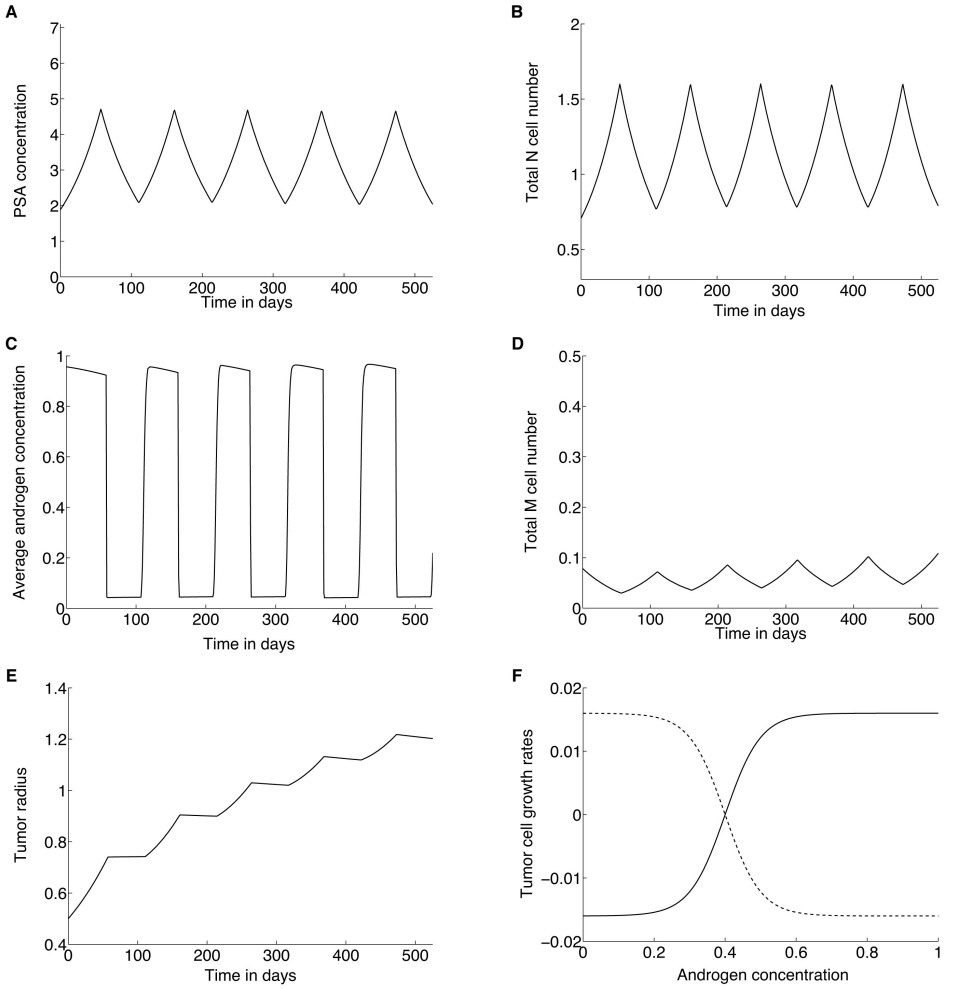

FIGURE 7. Numerical illustration of the case when intermittent androgen ablation is predicted to effect a cure. Intermittent treatment is based on the schedule that the time on therapy is 2 months and the time off therapy is 4 months. Figure shows time-courses of **A**, PSA concentration ($P(t)$), **B**, total number of androgen dependent cells ($=\int_{\Omega(t)} N(r,t)dr$), **C**, average androgen concentration ($=\int_{\Omega(t)} A(r,t)dr/\int_{\Omega(t)} 1dr$), **D**, total number of castration resistant cells ($=\int_{\Omega(t)} M(r,t)dr$), and **E** tumor radius ($R(t)$). **F**, Growth rates of androgen dependent cells (solid curve) and castration resistant cells (dashed curve).

Our model is formulated by a system of hyperbolic partial differential equations describing the spatio-temporal dynamics of various cellular species, coupled to an elliptic equation describing androgen dynamics. This resulted in a free boundary problem for the growing tumor. We began our model analysis by establishing existence and uniqueness of solutions for small time intervals when the tumor was

assumed to have a smooth boundary. For the radially symmetric case, existence and uniqueness of solutions with a continuously differentiable boundary were proved for all time.

Finally, numerical simulations of a tumor growing in 2-dimensions with radial symmetry were presented to illustrate tumor responses to different treatment strategies. We considered the case when castration resistant cells are androgen-repressed, that is, they have a negative growth rate when androgens are present in abundance. Our results showed that continuous therapy is predicted to result in treatment failure in finite time. The success or failure of intermittent therapy was found to be dependent on the growth characteristics of castration resistant cells, with the model able to reproduce clinically observed responses to therapy including failure in finite time, infinite cycling of PSA, and tumor remission.

These examples underscore the potential of our model to develop into a valuable tool that clinicians can use in making informed treatment choices. For this, the model needs to be extensively validated against patient treatment data, and requires the measurement of additional biomarkers such as cancer cell proliferation and death rates, and PSA expression levels per cell. Additionally, the simulation results for the radially symmetric case suggest several interesting mathematical problems:

1. Prove that under continuous androgen ablation (Figure 2) and under intermittent androgen ablation (Figure 3), the tumor radius $R(t) \to \infty$ as $t \to \infty$, and that the growth is faster under the latter protocol.
2. Prove that for tumor cell growth rates as in Figure 6F, the tumor radius $R(t)$ has the oscillator behavior suggested in Figure 6E, dependent on the scheduling of therapy.
3. The simulations in Figure 7 suggest the possibility of a 'cure' for certain treatment protocols, that is, $R(t)$ remains bounded as $t \to \infty$. Is there a limit which is a stationary solution of the system (P)?

Acknowledgments. The authors thank Dr Holger Perfahl for many helpful discussions. This research has been supported in part by the Mathematical Biosciences Institute and the NSF (grant DMS 0931642).

REFERENCES

[1] D. B. Agus, C. Cordon-Cardo, W. Fox, M. Drobnjak, A. Koff, D. W. Golde and H. I. Scher, *Prostate cancer cell cycle regulators: Response to androgen withdrawal and development of androgen independence*, J. Natl. Cancer. Inst., **91** (1999), 1869–1876.

[2] G. L. Andriole, E. D. Crawford, R. L. Grubb III, S. S. Buys, D. Chia, T. R. Church, M. N. Fouad, E. P. Gelmann, P. A. Kvale, D. J. Reding, J. L. Weissfeld, L. A. Yokochi, B. O'Brien, J. D. Clapp, J. M. Rathmell, T. L. Riley, R. B. Hayes, B. S. Kramer, G. Izmirlian, A. B. Miller, P. F. Pinsky, P. C. Prorok, J. K. Gohagan and C. D. Berg, *Mortality results from a randomized prostate-cancer screening trial*, N. Engl. J. Med., **360** (2009), 1310–1319.

[3] R. R. Berges, J. Vukanovic, J. I. Epstein, M. CarMichel, L. Cisek, D. E. Johnson, R. W. Veltri, P. C. Walsh and J. T. Isaacs, *Implication of cell kinetic changes during the progression of human prostatic cancer*, Clin. Cancer Res., **1** (1995), 473–480.

[4] G. Birkenmeier, F. Struck and R. Gebhardt, *Clearance mechanism of prostate specific antigen and its complexes with alpha2-macroglobulin and alpha1-antichymotrypsin*, J. Urol., **162** (1999), 897–901.

[5] X. Chen and A. Friedman, *A free boundary problem for elliptic-hyperbolic systems: An application to tumor growth*, SIAM J. Math. Anal., **35** (2003), 974–986.

[6] M. L. Cher, G. S. Bova, D. H. Moore, E. J. Small, P. R. Carroll, S. S. Pin, J. I. Epstein, W. B. Isaacs and R. H. Jensen, *Genetic alterations in untreated metastases and androgen-independent prostate cancer detected by comparative genomic hybridization and allelotyping*, Cancer Res., **56** (1996), 3091–3102.
[7] M. W. Dunn and M. W. Kazer, *Prostate cancer overview*, Semin. Oncol. Nurs., **27** (2011), 241–250.
[8] S. E. Eikenberry, J. D. Nagy and Y. Kuang, *The evolutionary impact of androgen levels on prostate cancer in a multi-scale mathematical model*, Biol. Direct, **5** (2010), 24–52.
[9] B. J. Feldman and D. Feldman, *The development of androgen-independent prostate cancer*, Nat. Rev. Cancer, **1** (2001), 34–45.
[10] A. Friedman, *A multiscale tumor model*, Interface. Free Bound., **10** (2008), 245–262.
[11] D. Gillatt, *Antiandrogen treatments in locally advanced prostate cancer: are they all the same?*, J. Cancer Res. Clin. Oncol., **132** (2006), S17–S26.
[12] R. F. Gittes, *Carcinoma of the prostate*, N. Engl. J. Med., **324** (1991), 236–245.
[13] M. Gleave, S. L. Goldenberg, N. Bruchovsky and P. Rennie, *Intermittent androgen suppression for prostate cancer: Rationale and clinical experience*, Prostate Cancer Prostatic Dis., **1** (1998), 289–296.
[14] S. L. Goldenberg, N. Bruchovsky, M. E. Gleave, L. D. Sullivan and K. Akakura, *Intermittent androgen suppression in the treatment of prostate cancer: A preliminary report*, Urology, **45** (1995), 839–844.
[15] M. A. Haider, T. H. van der Kwast, J. Tanguay, A. J. Evans, A. Hashmi, G. Lockwood and J. Trachtenberg, *Combined T2-weighted and diffusion-weighted MRI for localization of prostate cancer*, AJR Am. J. Roentgenol., **189** (2007), 323–328.
[16] Y. Hirata, N. Bruchovsky and K. Aihara, *Androgen receptor in prostate cancer*, Endocr. Rev., **25** (2004), 276–308.
[17] C. A. Heinlein and C. Chang, *Development of a mathematical model that predicts the outcome of hormone therapy for prostate cancer*, J. Theor. Biol., **264** (2010), 517–527.
[18] A. M. Ideta, G. Tanaka, T. Takeuchi and K. Aihara, *A mathematical model of intermittent androgen suppression for prostate cancer*, J. Nonlinear Sci., **18** (2008), 593–614.
[19] T. L. Jackson, *A mathematical model of prostate tumor growth and androgen-independent relapse*, Discrete Cont. Dyn.-B, **4** (2004), 187–201.
[20] T. L. Jackson, *A mathematical investigation of the multiple pathways to recurrent prostate cancer: Comparison with experimental data*, Neoplasia, **6** (2004), 697–704.
[21] H. V. Jain, S. K. Clinton, A. Bhinder and A. Friedman, *Mathematical modeling of prostate cancer progression in response to androgen ablation therapy*, Proc. Natl. Acad. Sci. USA, **108** (2011), 19701–19706.
[22] H. V. Jain and A. Friedman, *Modeling prostate cancer response to continuous versus intermittent androgen ablation therapy*, Discrete Cont. Dyn.-B, in press.
[23] M. Marcelli, W. D. Tilley, C. M. Wilson, J. E. Griffin, J. D. Wilson and M. J. McPhaul, *Definition of the human androgen receptor gene structure permits the identification of mutations that cause androgen resistance: premature termination of the receptor protein at amino acid residue 588 causes complete androgen resistance*, Mol. Endocrinol., **4** (1990), 1105–1116.
[24] H. C. Monro and E. A Gaffney, *Modelling chemotherapy resistance in palliation and failed cure*, J. Theor. Biol., **257** (2009), 292–302.
[25] W. D. Nes, Y. O. Lukyanenko, Z. H. Jia, S. Quideau, W. N. Howald, T. K. Pratum, R. R. West and J. C. Hutson, *Identification of the lipophilic factor produced by macrophages that stimulates steroidogenesis*, Endocrinology, **141** (2000), 953–958.
[26] T. Portz, Y. Kuang and J. D. Nagy, *A clinical data validated mathematical model of prostate cancer growth under intermittent androgen suppression therapy*, AIP Advances, **2** (2012), 011002.
[27] L. K. Potter, M. G. Zager and H. A. Barton, *Mathematical model for the androgenic regulation of the prostate in intact and castrated adult male rats*, Am. J. Physiol. Endocrinol. Metab., **291** (2006), E952–E964.
[28] A. S. Wright, L. N. Thomas, R. C. Douglas, C. B. Lazier and R. S. Rittmaster, *Relative potency of testosterone and dihydrotestosterone in preventing atrophy and apoptosis in the prostate of the castrated rat*, J. Clin. Invest., **98** (1996), 255–263.
[29] M. Yang, P. Jiang, F-X. Sun, S. Hasegawa, E. Baranov, T. Chishima, H. Shimada, A. R. Moossa and R. M. Hoffman, *A fluorescent orthotopic bone metastasis model of human prostate cancer*, Cancer Res., **59** (1999), 781–786.

[30] C. Y-F. Young, B. T. Montgomery, P. E. Andrews, S. Qiu, D. L. Bilhartz and D. J. Tindall, *Hormonal regulation of prostate-specific antigen messenger RNA in human prostatic adenocarcinoma cell line LNCaP*, Cancer Res., **51** (1991), 3748–3752.
[31] K. Yörükoglu, S. Aktas, C. Güler, M. Sade and Z. Kirkali, *Volume-weighted mean nuclear volume in renal cell carcinoma*, Urology, **52** (1998), 44–47.
[32] H. Y. E. Zhau, S. Chang, B. Chen, Y. Wang, H. Zhang, C. Kao, Q. A. Sang, S. J. Pathak and L. W. K. Chung, *Androgen-repressed phenotype in human prostate cancer*, Proc. Natl. Acad. Sci. USA, **93** (1996), 15152–15157.

Received October 17, 2012; Accepted December 26, 2012.

E-mail address: afriedman@math.osu.edu
E-mail address: hjain@fsu.edu